MICHIGAN STATE UNIVERSITY

CYCLOTRON LABORATORY

# EXTREME STATES IN NUCLEAR STYSTEMS

D. K. SCOTT

DECEMBER 1981

MSUCP-364

MSUCP-364
December 1981

# EXTREME STATES IN NUCLEAR SYSTEMS

*" Les extrèmes se touchent..."*
*L.-S. Mercier, Tableau de Paris*

D.K. Scott
National Superconducting Cyclotron Laboratory
and
Departments of Physics and Chemistry
Michigan State University
East Lansing, Michigan 48824, USA

ABSTRACT: Extreme states in nuclear systems are discussed in terms of limiting phenomena. Eight limits are described, viz. of angular momentum, reaction mechanisms, nuclei, space and time, temperature, density and matter. These limits have become accessible mainly through collisions of heavy nuclei, at incident energies ranging from a few MeV/nucleon up to energies of TeV/nucleon.

## INTRODUCTION

It is probably no exaggeration to say that there are few, if any, extreme states in nuclear systems (1). Rather there exist extreme points of view. Many of these are familiar and, indeed, have played a pivotal role in the development of nuclear science. For many years our ideas about nuclear reactions were dominated by compound and direct processes--extremes of time scale ranging from $10^{-16}$ to $10^{-23}$ sec. The coexistence of the shell and liquid drop models demonstrates the extremes of single particle and collective aspects. More recently we have seen both time-dependent Hartree Fock and nuclear hydrodynamical theories applied with some success to the dynamics of nuclear collisions, although the two theories start from paradoxically opposing hypothesis, the extremes of infinite and zero mean free path of a nucleon in the nucleus, and the extremes of few and many particle collisions. There is, however, a danger in associating these extreme viewpoints with extreme states, just as there is a danger in associating God with singularities in the solution of differential equations. With improved mathematics the singularities sometimes disappear. Similarly with improved nuclear theory, the extreme viewpoints disappear; complete extended shell model calculations, for example, exhibit collective features. As expressed succinctly by L.-S. Mercier in Tableau de Paris, "Les extrèmes se touchent". But before the extremes meet, they

serve as an invaluable focus for experimentalist and theorist alike, thereby accelerating our understanding of nuclear systems. The existence of enhanced BE2 transitions in the complexity of modern, extended shell model calculations would probably have gone unnoticed for a long time without the insight afforded by the earlier collective model.

## THE SEARCH FOR THE LIMITS

For these reasons, it is preferable to discuss extreme states in terms of various observed limits; in this paper I shall deal with eight limits, constituting an eight-fold path to our knowledge of nuclear systems. These limits are in Angular Momentum, Reaction Mechanisms, Nuclei, Time and Space, Temperature, Density and Matter. Like Galileo, I shall stick to "harsh, stubborn, irreducible facts", by selecting examples with at least some corroboration by experiment, and omitting the many imaginative, theoretical speculations spawned by the study of nuclear collisions.

By and large it is through the capability of modern accelerators to produce nuclei across the whole periodic table from energies at the barrier up to speeds approaching the velocity of light that researchers have discovered most of the limits. Some representative accelerators are shown in Fig. 1, by the maximum obtainable energy as a function of the Z of the accelerated particle. The first decade from 1 to 10 MeV/nucleon contains many accelerators, of which only the broad range SuperHilac is represented. From 10 MeV/nucleon to 10 GeV/nucleon, there are also many accelerators recently completed or under construction; a substantial part of the motivation behind the creation of these machines is the search for extreme states in nuclear systems. Beyond these accelerators there are bold proposals like VENUS (Variable Energy Nuclear Synchrotron) which, by colliding beams of nuclei at 20 GeV/nucleon, would be equivalent to the acceleration of nuclei on a fixed target at 1 TeV/nucleon (1). At such energies two uranium nuclei are contracted to a diameter less than that of a single nucleon, giving the possibility of depositing tremendous amounts of energy into a tiny volume. The number of emergent particles is expected to number in the thousands, creating an extreme state in which it would be true to say that never in the history of human endeavor was so much produced from so little with such force in such a short time and at such a great expense. Ultra-relativistic collisions will be our only means of reconstructing in the laboratory the conditions prevailing in the first instants following the origin of the universe with the Big Bang. In the future, these experiments may lead to the ultimate characteristic extreme shown on the right of Fig. 1 by the synthesis of nuclear, particle and astrophysics in

Cosmology. Some intimations of the possibilities may be forthcoming from experiments already underway with colliding alpha particles in the Intersecting Storage Rings (ISR) at CERN. As Fig. 1 shows, the equivalent fixed target energy obtained is about 0.5 TeV/nucleon. These experiments will also help to bridge two extreme viewpoints; the $\alpha$-particle is considered too light by heavy ion scientists but too complicated by the particle physicists. For this reason alone, the experiments are likely to be of value!

The eight limits we shall discuss are shown in Fig. 1, located approximately in energy domains where experiments have already contributed to their demarcation. In progressing form the bottom to the top of the energy scale, various thresholds are passed, for example the sound velocity, the Fermi energy, the pion and strangeness thresholds. At these points the characteristic physics can change. At opposite ends of this scale the differences in our views of nuclear collisions are certainly extreme, as symbolized in Fig. 2. Collisions of nuclei at low energies, below 10 MeV/nucleon, reveal the detailed spectroscopy of interweaving levels, which are arranged in rotational and vibrational bands. The intricacy and complexity can be compared to a cathedral, with its delicate tracery, arches, tapestries and icons. Compare the explosive outcome of shattering a nucleus with a high speed argon projectile traveling close to the velocity of light. It is as if a bomb was dropped in the cathedral! This technique is not suited to the study of delicate tracery. Rather one delivers a short, sharp blow to the nucleus, and then measures its response to shock and stress. In describing the same nucleus we use language which deals with the symmetries of the interacting boson model and with the tensile strength and viscosity of nuclear matter, so that extreme and paradoxical approaches to the nucleus are as prevalent today as they have been in the past. Although parts of the nuclear community seem to be disillusioned with either extreme, both appear to be necessary - to discover how the nucleus is put together and how it comes apart.

## THE LIMITS OF ANGULAR MOMENTUM

Faced with the complexity of Fig. 2, it is natural to search for simplicities (2). The excitation energy of a typical rotational nucleus with A=164 as a function of angular momentum is illustrated in the top part of Fig. 3. As the nucleus rotates faster it begins to deform, becoming more prolate. The excitation energy can be expressed,

$$E_J = \frac{h^2}{2I} J(J+1)$$

with $I$ the moment of enertia. Close examination "under a magnifying glass" shows that there occur sudden discontinuities. The magnification is realized in practice by plotting the moment of inertia as a function of the square of the rotational frequency in the bottom part of the figure. When the speed of rotation increases, the coriolis forces cause the alignment of the angular momentum of two ($i_{13/2}$) particles with the rotation axis. A small tremor takes place in the nucleus, which rearranges its shape under the stress. The alignment of the particles causes a bulge around the equator, increasing the moment of inertia and decreasing the rotational frequency as the angular momentum is redistributed between collective and independent particle degrees of freedom. This first rearrangement takes place at $J \approx 14\hbar$. At $28\hbar$, an angular momentum which can easily be realized in a heavy ion collision, another accomodation to the stress occurs as two ($h_{11/2}$) particles break off and align, creating a second "back-bend". The successive alignment of single particles causes the nucleus to evolve in shape from prolate to oblate, and eventually leads to an extreme where the angular momentum is largely carried by single particle motion. In the upper figure the effect of these backbends appears as a "band-crossing", where a new rotational band with a larger moment of inertia, and therefore a less steep slope, cuts across the lower band. The ultimate band-crossing, or "superbackbend", occurs when the yrast line is crossed by the locus of the rotating fission configuration. Al low angular momentum this saddle shape lies some 30 MeV above the ground state, constituting the fission barrier. The larger moment of inertia of this shape ensures that it must intercept the ground state band, a crossing which occurs at $J \approx 80\hbar$. In the bottom figure there is evidence for this superbackbend at the much lower J-value of about $55\hbar$. Although the reason for the lowering is not well understood (3), it appears, however, that an extreme has been reached, marking the limit of the rotational motion of a nucleus.

A powérful and elegant means of portraying these shape changes of the nucleus is given in Fig. 4. Here the number of coincidences between successive $\gamma$-rays transitions in the bands is plotted in a contour diagram (2). If the rotational sequence were smooth and well behaved, no two $\gamma$-transitions could have the same energy, since $E_J \propto J(J+1)$, and therefore $\Delta E_J \propto J$. A diagonal valley is created in the plot, devoid of counts, due to the absence of equal energy transitions. In the region of a backbend, several transitions of equal energy can occur, which therefore fill in the valley with bridges. This type of plot, with its many side ridges, plateaux, and other contours is a rich goldmine of information about the shape changes of a nucleus under the stress of angular rotation.

This technique can be extended to more than two γ-rays in coincidence by using a multiplicity array of detectors. Present designs contain up to about 150 detectors, the precise number being circumscribed by Pythagorean theorems for accomodating pentagons and hexagons on the surface of a sphere. An example of one device (4) is illustrated in Fig. 5. It is beyond the power of the human mind to visualize the subtleties of the 2-D patterns of Fig. 4 extended to a multidimensional space, but it is not beyond the power of mathematics. We can, however, readily appreciate the power this instrument brings to the study of the limits of angular momentum.

## SOME LIMITS OF REACTION MECHANISMS

A classification of various reaction processes (5) in nuclear collisions is set out in Fig. 6. The top half shows the main paths which are followed, with the extremes of direct and compound nuclear reactions as the two outermost routes. These processes encompass extremes of time from $10^{-22}$ to $10^{-16}$ sec., as well as extremes of simplicity and complexity; in a direct reaction the identity of the initial state is largely preserved, but it is obliterated in the compound nuclear process. These reactions are also associated with the extremes of peripheral and central collisions, involving large and small angular momentum and impact parameter. The two mechanisms occupy the ends of a plot of reaction cross section as a function of angular momentum, circumscribed by the unitarity limit, $\sigma_\ell = \pi\lambda\!\!\!^{-2}(2\ell+1)$, shown in the bottom half of Fig. 6, but the extremes do, however, meet through other intermediate reaction mechanisms. As we have seen, beyond a critical angular momentum, denoted $\ell_f$, a new path opens through the fission channel in which the compound nucleus disintegrates into roughly equal mass fission fragments. Instead of a spherical compound nucleus, the intermediate system takes on the saddle shape. The fission process occurs on a faster time scale, carving out its own territory in reaction space. A new process of deep inelastic scattering bridges the remaining gap to the direct reaction. Here a rotating dinuclear complex is formed which lasts for $10^{-21}$ - $10^{-22}$ sec. before separating into nuclei more reminiscent of the initial channel than are the symmetric fission fragments. The associated reaction space begins at a critical angular momentum, $\ell_c$, which is so high that the balance of the attractive nuclear forces and the disruptive centrifugal and Coulomb forces does not allow the nuclei to come close enough to form the compound or saddle shape system. Like the city of Instanbul, this process stands as a bridge between two different continents, containing something of the characteristics from each. There appears to exist a hierarchy of extremes with finer and finer divisions. Very recently a new process of fast fission, occurring on a time scale of

$10^{-20}$ sec., may have been discovered, subdividing once more the space between fission and deep-inelastic scattering (5).

The study of deep-inelastic scattering has preoccupied many nuclear scientists, experimentalists and theorists alike, for the last ten years. The evolution of a small quantum mechanical system can be followed in time through the angle of rotation of the dinuclear system, and the progress towards equilibrium of various collective degrees of freedom such as energy, angular momentum, mass asymmetry, neutron-proton excess can be measured. The driving force for this evolution comes from the potential energy, which is shown in Fig. 7 as the energy surface E(Z,A) of nuclei (in the region of Xenon), calculated with the liquid droplet model. Due to the (A-2Z) charge symmetry term in the formula this potential surface has a steep valley in the (N-Z) direction, whereas the slope is very gentle in the orthogonal direction of the mass asymmetry coordinate. Deep inelastic studies have mapped out the path taken by a nuclear system injected onto this surface, e.g. the $^{56}Fe + ^{136}Xe$ system illustrated. Of the many possible routes, the nuclei prefer the fastest route to the bottom of the steep valley, thereby equilibrating the N/Z degree of freedom. Neutrons and protons are exchanged on a fast time scale of $10^{-22}$ sec., tending to equalize the N/Z ratio to a common value. Thereafter the system slowly eases down the mass asymmetry valley, until eventually $N_1 = N_2$ and $Z_1 = Z_2$. The markers along the path denote the amounts of initial collective energy dissipated into intrinsic excitation of the dinuclear system, and is a rough measure of elapsed time from injection. The energy conversion takes place largely by the same process of nucleon exchange that is responsible for equilibrating the other degrees of freedom. Since large amounts of energy are dissipated rapidly, this reaction mechanism was given the name deep inelastic scattering, or more correctly deeply-inelastic scattering; it is the inelasticity which is large, rather than the depth of the scattering!

The path chosen by the system is an extreme one, dominated by the random walk of statistical diffusion. As illustrated in Fig. 7, the system could have overshot the valley, performing quantal oscillations of giant multipole modes, but the motion appears to be so overdamped that most nuclei do not behave in this way.

Shell effects give rise to "magic holes", or pock-marks, on the smooth energy surface. A goal of much heavy ion research is to get the nuclei into the extreme magic holes of the superheavy elements. As anyone who plays golf knows, it is difficult to get balls into holes on a surface which

slopes in many directions, and so far no attempts have been successful. To make the game even harder, one cannot any longer by sure that the holes exist! The game will continue to be played; without the Holy Grail of superheavy elements, it is clear that in the excursions over the landscape of Fig. 7, a wide range of nuclei with new values of Z and N become accessible.

## THE LIMITS OF NUCLEI

The limits of nuclei lie far beyond our present knowledge (6,7). Fig. 8 shows the 300 or so naturally occurring stable nuclei, together with the approximately 1600 additional radioactive nuclei that have been discovered over the last 50 years of nuclear research. Well beyond lie the theoretical limits of nuclear stability containing another 6,000 or so nuclei expected to be stable against decay on a strong interaction time scale. The properties of these nuclei constitute a rich field for speculation. They will give rise to new shapes, new decay modes, new regions of closed shells, of collective deformation, and possibly of new densities. It is conjectured that extremely neutron excess nuclei may assume configurations quite different from our familiar experience. Toroidal and poly-centered nuclei are theoretically possible forms. In $^{70}Ca$, for example, the neutrons may group into polyneutron clusters around the outside of a normal configuration (8). The most promising means of checking these ideas, indeed in many cases the only means, is the collision of heavy nuclei.

In Fig. 9 some of the highlights in the study of exotic nuclei far from stability over the last year are displayed (6,9). New regions of closed shells at $Z \simeq 40$ and 64 with $N \approx 50$ and 82 have been found, as well as new regions of deformation. New decay modes have been discovered, including delayed two-and three-neutron activity, and a new region of alpha radioactive nuclei extending out to the proton drip line. In addition to the well known $\beta$ and $\gamma$ radioactive decay modes, a new mode of proton decay from the ground state of $Lu^{151}$ was discovered, the first to be added since Rutherford's day (10). Progress in the synthesis of new elements took a step forward by the cold fusion of $^{54}Cr$ on $^{209}Bi$ emitting one neutron to make element Z=107 with A=262.

It is, however, the neutron rich nuclei that present the most challenging limit, because they lie so far beyond our present knowledge. The nuclear debris produced in a high energy nuclear collision, such as that depicted in Fig. 2, seems to be a copious source of these exotic fragments (11). The diagonally shaded neutron rich nuclei in Fig. 10 were produced either by

this means or by the lower energy deeply inelastic process discussed earlier. Together, these two methods have made a substantial advance towards the limit of neutron rich nuclei, and in all likelihood will reach the boundary within a few years.

## SPATIAL AND TEMPORAL LIMITS

The limits we have discussed so far are concerned with rather mild perturbations of the nucleus; now we consider more drastic processes. The two extremes are illustrated in Fig. 11. On the left is a collision of $^{16}O$ on $^{40}Ca$ according to a time dependent Hartree-Fock calculation at a low incident energy (12). The composite system has time to adjust in a smooth fashion as the single particle wave functions accomodate themselves to the changing mean field. As in the static shell model, the single particle motion is governed by the exclusion principle, which allows very long mean free paths. (In the figure the limit of $\lambda=\infty$ is indicated.) The conditions in the high energy collision on the right are quite different (13), since there is insufficient time for nuclear rearrangement. The overlapping portions of the nuclei constitute a violent participant zone, which moves with a velocity intermediate between those of the residual spectator fragments. These are sheared off the parent nuclei, leaving a projectile fragment continuing with approximately the original beam velocity and a target fragment sitting almost at rest. The participants and sepctators constitute a new class of objects in nuclear collisions. The case illustrated in Fig. 11 is the outcome of a hydrodynamical model, which starts from the assumption of a short mean free path, just the opposite extreme of the TDHF theory. Once again we see, side by side, two paradoxical and antithetical extreme views of a nuclear system. With further theoretical developments, these extremes too will surely meet, as the addition of two body collision terms into the TDHF approximation gives rise to aspects of the hydrodynamical model. These collision terms become important at high bombarding energies, due to the diminished influence of the Pauli exclusion effects.

This high energy collision gives us information on spatial and temporal limits. The participant region is a spatially localized zone, a subvolume of the nuclear system into which large amounts of energy can be deposited. The dimensions of the zone have been determined using two particle interferometry, borrowing a technique for measuring the size of stars by the Hanbury-Brown and Twiss method (14). Within this nuclear fireball, limits of temperature and density may become accessible whereas temporal limits can be measured in the spectators. An excellent description of the

creation of spectators and participants is found in the works of Dante with the lines, "The act is done 'ere time has time to flow". The abrasion process is over before the nucleus has time to adjust.

The spectators give us a snapshot of the zero-point, ground state motion of the fragments in the parent nuclei, not only of the nucleonic motion but also of large clusters, through a measurement of the momentum distributions (15). The momentum widths of all fragments can be reduced to an effective width associated with the nucleonic motion, denoted by $\sigma_o$, of which the values derived from experiments with $^{12}C$, $^{16}O$ and $^{40}Ar$ projectiles over an incident energy range from 40 MeV/nucleon to 2 GeV/nucleon are shown by the right hand scale in Fig. 12. The average value ≈90 MeV/c is smaller than the value $P_f/\sqrt{5}$ expected for an uncorrelated Fermi ground state motion, suggesting the presence of correlations. The uniform behaviour of the momentum distribution also indicates that the spectator process may be identified at quite low incident energy of 40 MeV/nucleon. A more precise limit, which would also delineate the transition between mean field and hydrodynamical phenomena, remains to be determined. In the next two sections we leave our discussion of the spectators and turn to limiting phenomena in the more extensively studied, and possibly more exciting, participants.

## THE LIMITS OF TEMPERATURE

There are many novel properties of the participant zone in Fig. 11 to be studied, but one of the simplest is the global parameter of temperature. It has been extracted from the energy spectra of emitted light particles e.g. of protons, neutrons and, at energies above several hundred MeV/ nucleon, of pions. The results for a variety of systems are plotted in Fig. 12 using the scale at the left (16). As the incident energy increases, more energy is pumped into the localized zone and, not surprisingly, the temperature rises, but not indefinitely. From the results of p+p and $\alpha+\alpha$ collisions at energies close to 1 TeV/nucleon, the measured temperature--as determined from the transverse momentum distributions--appears to limit (15,16). (In the case of p+p collisions, an hadronic fireball is created rather than a nuclear fireball.)

The limit is almost certainly due to particle creation in the fireball. With increasing energy it becomes easier to create new particles than to add additional random kinetic energy to the old (17). In the special case of an exponentially increasing density of particle states in nature, the temperature saturates at approximately 140 MeV. Since the phenomenon has a

mathematical analogy with the boiling of a liquid, the limiting temperature is sometimes called the "boiling point of hadronic matter". There are several possibilities for generating an exponential particle spectrum, for example the bootstrap model. The temperature variation for three possible elementary particle worlds including the exponential spectrum is shown in Fig. 13; if the finite number of presently known particle states constituted the complete set, the temperature would of course increase indefinitely, as it would also in the case of a quark model, incorporating only the valence quarks. However, if the sea of quark-antiquark pairs is included, the temperature could also limit, just as in the case of the exponential spectrum. Unfortunately it is not yet possible to say that the observed limit of the temperature conveys unambiguous information about the ultimate spectrum of particle states, since the measured temperatures are not those reached initially in the fireball, but the result of an expansion and cooling process (18). The predicted initial temperature (12) in Fig. 13 is certainly higher than the measured value, but it seems that the asymptotically observed temperatures would be rather similar for a completely different set of initial conditions (18). In the lower energy region the temperature shown in Fig. 13 corresponds to treating the participant zone as a Fermi gas with equal contributions from the target and projectile (19). As in the case of the spectators, it appears that the spatially localized hot zone can be isolated down to energies of 40 MeV/nucleon; at this energy the collision velocity is close to the intrinsic Fermi velocity, $v_F$, shown on the figure, which could turn out to be a necessary condition for the onset of the participant-spectator geometry.

## THE LIMITS OF DENSITY

In addition to creating high temperatures the fireball is also a potential source of high density nuclear matter. Various conjectures on limiting states of matter as a function of T and $\rho$ are illustrated in Fig. 14. Either high T or high $\rho$ is sufficient to create the quark matter phase, when the individual hadron bags are forced in one large quark bag.

Moderately high densities of about 4 times normal nuclear matter density might also induce a phase transition to a pion condensate, which is an ordered state containing many pions, provided the temperatures are not simultaneously too high. The calculated loci of temperature and density for two typical nuclear collisions as a function of time are shown, from which we see that the low energy collision of 0.5 GeV/nucleon $^{40}Ar$ on $^{40}Ca$ appears to be most promising. The problem, however, is to identify an

experimental signature for the formation of this new phase of nuclear matter.

Firstly it is necessary to establish experimentally that higher than normal density is achieved during a nuclear collision, since the validity of hydrodynamical models for a significant fraction of the cross section is by no means universally accepted. The best evidence (20) is summarized in Fig. 15, in which the top and bottom panels compare the predictions of hydrodynamics and the cascade model for the emitted spectrum of protons in the collisions of $^{20}$Ne on U at 393 MeV/nucleon. According to Fig. 14, at this energy compressions of 4 should be achieved, which in the hydrodynamical model lead to a side splash of protons at an angle of $70^{o}$-$90^{o}$ (see bottom right panel). On the other hand, the intranuclear cascading, which treats the collision as a succession of individual nucleon-nucleon interactions, does not produce as much sideways peaking of the emitted particles (see top left panel). The experimental data shown in the left hand middle panel exhibit a sidewards peaking (the different curves correspond to different emitted proton energies) and in fact appear to agree rather well with a more elaborate hydrodynamical calculation including evaporation.

There is now considerable investment of time, effort and money into the detection of the possible phase transitions that might accompany the high density conditions. One of the extreme devices is illustrated in Fig. 16, both schematically and in reality. It consists of an array of 800 detectors surrounding the target to detect the splash and flow pattern of emitted particles, which are measured in coincidence with leading particles in a down stream array, or wall, of 100 plastic scintillators. These can be used to single out the central collisions and the most catastrophic events. Like the high multiplicity $\gamma$-ray apparatus, which we mentioned in the discussion of angular momentum, this device heralds a new era in experimental nuclear physics, by itself an extreme, of making high multiplicity, exclusive measurements and of total event reconstruction (21).

Since results with this apparatus are not yet available, it is appropriate to recall some intriguing observations with nuclear emulsions, in which splash angles similar to those of Fig. 15 were also measured. The variation of this angle with incident energy (13) is shown in Fig. 17, from which we see that the trend is rather different from the expectation of a simple--albeit outdated--hydrodynamical model; the angle increases with energy, and in the vicinity of 2 GeV/nucleon becomes ill-defined. This behaviour is expected in the case of a phase transition to a pion condensate or to a

density isomer (a related phase transition) when the nucleon-nucleon scattering cross section is greatly increased. These measurements will soon be repeated with the more sophisiticated electronic apparatus; however the results of emulsion and live detector experiments in the region of 400 MeV/nucleon appear to be in agreement, so there is hope that the emulsion experiments will be corroborated.

These results provide the sole direct evidence for an extreme state of matter due to a pion condensate or a density isomer. Other attempts to detect anomalous behaviour in the pion multiplicity distribution, in deviations from the random statistical background by a coherent signal, or of coherence in the localized participant source from measurements of two particle correlations, have failed to turn up positive evidence (14). However, it is also true that searches have not yet been carried out with large nuclei, such as uranium, which come closer to the idea of extended nuclear matter.

## THE LIMITS OF MATTER

In this last section we turn to the outermost area of Fig. 14, where at either very high temperature or very high density, quark matter may be formed. Several intriguing pieces of experimental data are believed by the optimists to give some hints of this phase.

In experiments with emulsions it is not unusual to find a sequence of star collisions, as illustrated in Fig. 18. Here a primary nucleus of iron at 1.5 GeV/nucleon interacts in the emulsion creating a star, from which a leading fragment of Z=24 emerges as a secondary. There follows a secondary interaction producing Z=20, and a tertiary leading to Z=11. The secondaries and tertiaries have the unusual property that 6% of the reaction cross section leads to nuclei with an interaction cross section 10 times greater than normal, and with a lifetime greater than $10^{-10}$ sec. (14,22). The increased cross section implies the existence of a force some three times greater in range than the normal strong interaction. These phenomena are also observed with $^{16}O$ beams, and possibly even with $\alpha$-particle beams. In the latter case the anomalous secondary fragments are deuterons. The unusual properties of the secondary particles have earned them the name "anomalons", and in the case of deuterons an explanation in terms of "demon deuterons" has been proposed (23).

The idea is illustrated in Fig. 19. In modern calculations, the ground state of a deuteron is characterized by a 93.8% bound np configuration, 0.6%

bound $\Delta\Delta$, and 5.6% of a 6 quark collective state, at an excitation of 270 MeV above the ground state. The two hadron bags are forced together into one large bag, creating a temporary state of quark matter, as a result of ground state fluctuations. In the high energy nuclear collision it is conjectured that this state is enhanced, producing a real state of quark matter. As indicated in the figure, one possible configuration for this novel state of matter is a quark rearrangement into an exotic color excitation of three color dipoles. Although from an external point of view this object is still a color singlet, it is internally polarized, and can give rise to very strong interactions. What we usually observe as the strong nuclear force is but the pale reflection of these strong interactions between quarks, just as the Van der Waals forces between electrically neutral molecules are a pale shadow of the electromagnetic forces between nuclei and electrons. Whether this explanation for anomalons is consistent with the observed lifetime of $10^{-10}$ sec is not at all obvious. Perhaps the most remarkable outcome of the experiments is their forcing theorists to come to grips in nuclear physics with the ever increasing reality of quantum chromodynamics. It has been suggested, for example, that the anomalous behaviour could also be due to fractional charges accompanied by unconfined gluon fields, tightly bound to nuclei because of the strong color polarizability of nuclear matter (24). In the currently accepted theory of strong interactions with quantum chromodynamics, these free charges are not allowed to exist.

The mechanism for forming the quark matter of the anomalons is quite unclear--assuming that the explanation is along the correct lines. According to Fig. 14, quark matter can be created at very high temperatures, when the individual hadrons lose their identity and dissolve into a quark-gluon plasma. This state of matter very likely existed in the first instants following the origin of the universe with the Big Bang (17). The requisite temperatures are much higher than the limiting hadronic temperature $\approx$140 MeV which we discussed earlier. According to Fig. 20 (top) as the quark plasma cooled, a phase transition to the hadron states took place at a critical temperature $T_c$. There exists skeletal experimental evidence for both phases in very high energy collisions (17).

The spectra of emitted pions in p+p collisions at high energies consist of two components (see bottom of Fig. 20). The low momentum part (0-1.5 GeV/c) has a constant slope of approximately 160 MeV, independent of incident energy, and is to be identified with the limiting temperature of the hadronic phase which we mentioned earlier. In addition the spectra contain a high momentum tail, the slope of which varies with incident energy

as $E^{2/7}$. One interpretation--though not the only one--is that the "preequilibrium" emission originates from the high temperature quark-gluon phase (17). If true, then these high energy collisions offer us the remarkable opportunity of investigating in the laboratory processes that occurred in the first $10^{-15}$ sec or so in the history of our universe. A comparison of hadronic and nuclear fireballs is also of great interest, since it allows the relative concentration of up and down quarks in the initial state to be varied. A preponderance of up and down quarks leads to characteristic production ratios of strange particles, e.g. $\bar{\Lambda}/\bar{p}$.

The condition of matter in the Big Bang certainly represents an extreme state of the most profound scientific and philosophical consequence. It also represents the last of the eight characteristic limits we set out to discuss in this paper. Throughout the history of nuclear science, it has been both necessary and constructive to introduce extreme and paradoxical models and viewpoints, which after some time begin to merge. From the discussion of the eight modern limits, it is clear that extreme views are just as much a part of nuclear studies now as they have been in the past. No doubt these too will be modified in time, and perhaps research on them should be regarded like the enigmatic experience in H. Mearns poem, the Psychoed,

"As I was going up the stair,
I met a man who wasn't there.
He wasn't there again today,
I wish, I wish he'd stay away.

Only the message of the last line is inappropriate - the study of extreme states and limiting phenomena, even if transitory, is an exciting and vital part of research in nuclear science.

ACKNOWLEDGEMENTS

While preparing this talk, I received advice and help on the selection and interpretation of topics from many people. In particular, I wish to thank W. Benenson, G. Bertsch, J. Boguta, J. Cerny, G. Chapline, E. Friedlander, C.K. Gelbke, N.K. Glendenning, H. Gutbrod, M. Gyulassy, H. Heckman, S. Nagamiya, A.M. Poskanzer, H.G. Pugh, D.G. Sarantites, P. Siemens, R. Stock, H. Stocker, G. Smith, F. Stephens, D. Strottman, H. Toki, P. Watson, G. Westfall and K. Wolf. It is also a pleasure to thank Patricia Pirnie and Betty Brewer for typing and assembling the manuscript as well as B. Decker, M. Blosser and the Staff of the Instructional Media Center for preparing the illustrations with great skill.

This material is based upon work supported by the National Science Foundation under grant no. PHY-80-17605.

REFERENCES


1. H.G. Pugh, Proc. of the Workshop on Future Relativistic Heavy Ion Experiments (GSI, Darmstadt 1980), Publication GSI 81-6, page 1.
2. F.S. Stephens, Nucl. Phys. A354 (1981) 289.
3. R.M. Diamond, Proc. of Int. Conf. on Nuclear and Atomic Physics with Heavy Ions (Bucharest, Romania, 1981), to be published.
4. D.G. Sarantites et al., Proc. of the Int. Conf. on Nuclear Behaviour at High Angular Momentum (Strasbourg, 1980), Suppl. J. de. Phys. FASC12 C10-1980, p. 269.
5. A. Gobbi, Nucl. Phys. A354 (1981) 337.
6. Proc. of 4th Int. Conf. on Nuclei far from Stability (Helsingor, Denmark 1981), CERN Publication 81-09.
7. B. Jonson, Nucl. Phys. A354 (1981) 77.
8. D.H. Wilkinson, Proc. of 3rd Int. Conf. on Nuclei far from Stability (Cargèse, 1976), CERN Publication 76-13, p. 71.
9. D.K. Scott, Summary Talk for Int. Conf. on Nuclear Atomic Physics with Heavy Ions (Bucharest, Romania, 1981), to be published.
10. G. Munzenberg et al., Z. Phys. A300 (1981) 107.
11. T.J.M. Symons, Ref. 6, p. 668.
12. J. Negele, Proc. of Int. Conf. on Extreme States in Nuclear Systems (Dresden, 1979), ZfK Publication - 430, Vol. 2, p. 198.
13. H. Stocker, et al., ibid., Vol. 2, p. 23.
14. M. Gyulassy, Nucl. Phys. A354 (1981) p. 395.
15. D.K. Scott, Nucl. Phys. A354 (1981) p. 375.
16. K. Wolf, Proc. of 5th High Energy Heavy Ion Study (LBL, Berkeley, 1981), to be published.
17. R. Hagedorn, Proc. of Workshop on Future Relativistic Heavy Ion Experiments (GSI, Darmstadt 1980), Publication GSI 81-6, p. 236; ibid J. Rafelski, p. 282.
18. N.K. Glendenning and Y.J. Karant, Phys. Rev. 21 (1980) 1501.
19. D.K. Scott, Intermediate Energy Heavy Ion Collisions in Proc. of Int. Conf. on Nuclear and Atomic Physics with Heavy Ions (Bucharest, Romania, 1981).
20. H. Stocker et al., Proc. of 5th High Energy Heavy Ion Study (LBL, Berkeley, 1981), Abstracts LBL Publication 12652, p. 57.
21. R. Stock, Proc. of 5th High Energy Heavy Ion Study (LBL, Berkeley, 1981) to be published.
22. E.M. Friedlander et al., Phys. Rev. Lett. 45 (1980) 1084.
23. S. Fredriksson, Proc. of 5th High Energy Heavy Ion Study (LBL, Berkeley, 1981) to be published.
24. G.F. Chapline, Lawrence Livermore Laboratory Preprint UCRL-86444 (1981).

FIG. 1. The energy regions and possible characteristic extreme states or limits covered by recently constructed, as well as some proposed, heavy ion accelerators. In cases where several machines cover similar ranges, only one representative line is shown.

FIG. 2. Superposition of two extreme approaches towards the nucleus. The detailed level structure of $^{68}Ge$ studied in low energy collisions is contrasted with the complete disintegration into fragments of $^{40}Ar$ at 72,000 MeV in a nuclear emulsion.

FIG. 3. The yrast line of a nucleus (top) showing band crossings and shape changes at critical angular momenta. An extreme crossing occurs at the right where the fission barrier vanishes. The bottom figure magnifies the discontinuities by showing the moment of inertia as a function of rotational frequency squared.

FIG. 4. Contour display of coincidences between $\gamma$-rays in a collective rotational band, showing a diagonal valley devoid of counts, which is filled in at the points of discontinity of Fig. 3. The plot contains many other details of nuclear shapes at high angular momentum.

FIG. 5. A multiplicity array of seventy $\gamma$-ray detectors for the study of nuclei at high angular momentum.

FIG. 6. A classification of known heavy ion reaction mechanisms, according to the paths through the intermediate composite systems (top) and according to regions of angular momentum, time and impact parameter (bottom).

FIG. 7. The possible paths of evolution of a nuclear system $^{56}Fe + ^{136}Xe$ under the driving force of the liquid drop potential energy surface, shown as a function of Z, A in the vicinity of Xe.

FIG. 8. Chart of the nuclides, showing the nuclei stable in nature, the presently established limit of stability as well as the theoretical boundaries. Various possible decay modes are indicated.

FIG. 9. Recently discovered features of nuclei far from stability.

FIG. 10. Chart of the light nuclides, illustrating the recent advances to the limit of stability by means of heavy ion reactions. Deep inelastic and relativistic fragmentation reactions produced the diagonally shaded neutron excess nuclei.

FIG. 11. Extreme reaction mechanisms are illustrated by the time dependent Hartree-Fock calcuation of density profiles in low energy collisions on the left, and by a hydrodynamical calculation of temperature and density contours for a relativistic collision on the right.

FIG. 12. Evolution of properties of spectators and participants with incident energy. The zero-point motion of spectator fragments is illustrated by the momentum distributions (right scale) and the temperature of the hot, participant zone by the scale on the left. The region of 35 MeV/nucleon marked by the arrow indicates the lowest energy at which a participant-spectator picture is established. The limiting temperature of hadronic matter is shown, as well as a theoretical estimate of the initial fireball temperature.

FIG. 13. The theoretical variation of temperature with center of mass energy for three possible densities of elementary particle states.

FIG. 14. Possible phases of nuclear and hadronic matter as a function of density and temperature. The locus of $\rho$ and T as a function of time is shown for collisions at two energies in a cascade calcuation.

FIG. 15. Differential cross sections of emitted protons in the collision of $^{20}Ne$ on $^{238}U$ at 393 MeV/nucleon. The hydrodynamical calculation (bottom) gives splashing of protons to wider angles than does the cascade calculation (top), and in a more sophisticated version (middle right) is in better accord with the data (middle left). The different curves are for different energy bins of emitted protons.

FIG. 16. Large multiplicity array of about 1,000 detectors, shown schematically (left) and in reality (right), for the detection of emission patterns of light particles in heavy ion collisions.

FIG. 17. The observed angle of sideways splashing (see Fig. 15) as a function of incident energy for $^{16}O$ in emulsions, compared with a hydrodynamical calculation, and also with the inclusion of a phase transition to a density isomer.

FIG. 18. Illustration of secondary, tertiary and quartenary fragments from successive interactions in a nuclear emulsion, initiated by a primary Fe beam of 1.5 GeV/nucleon. A fraction of the particles have anomalously large interaction cross sections.

FIG. 19. A possible interpretation of anomalons, for the case of deuterons, by the formation of color polarized quark matter.

FIG. 20. Theoretical estimate (top) of the abundance of elementary particles in the early history of the Universe, from the quark-gluon plasma phase to the hadronic fluid phase. The emission of pions from hot fireballs in high energy proton collisions (bottom) is attributed to the two phases by the component of constant slope as the limiting hadronic temperature, and the preequilibrium higher temperature tail from the quark plasma phase.

MSUX-81-329

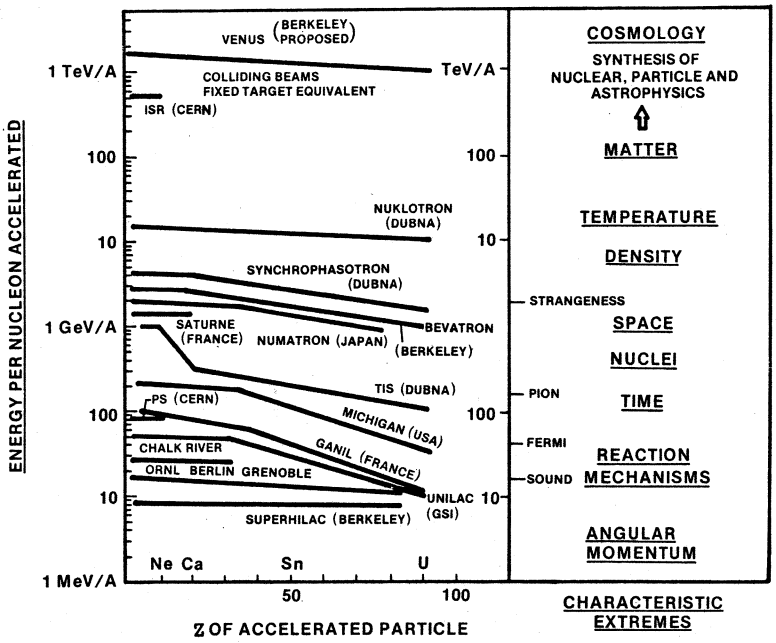


MSUX-81-318

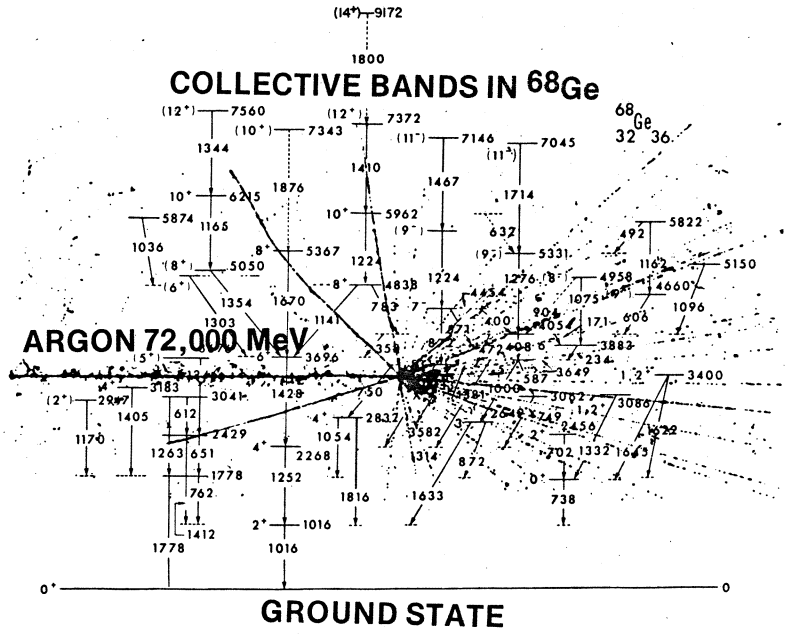

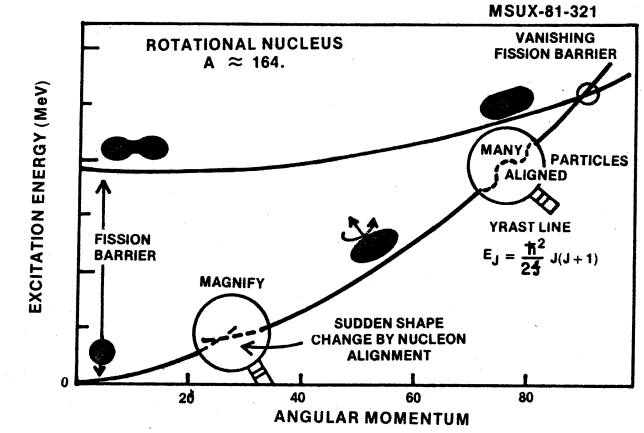
MSUX-81-321
ROTATIONAL NUCLEUS
A ≈ 164.
VANISHING
FISSION BARRIER
MANY
PARTICLES
ALIGNED
YRAST LINE
$E_J = \frac{\hbar^2}{2\mathcal{J}} J(J+1)$
FISSION
BARRIER
MAGNIFY
SUDDEN SHAPE
CHANGE BY NUCLEON
ALIGNMENT
EXCITATION ENERGY (MeV)
0
20
40
60
80
ANGULAR MOMENTUM

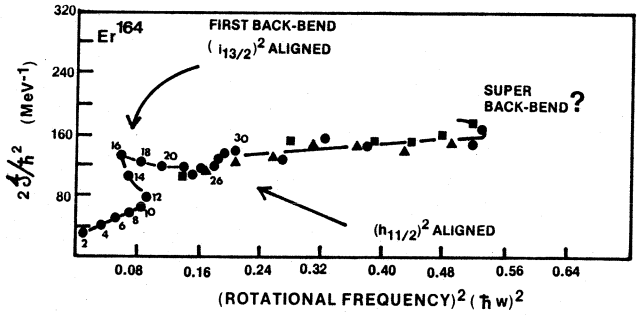
320
240
160
80
$Er^{164}$
FIRST BACK-BEND
$(i_{13/2})^2$ ALIGNED
SUPER
BACK-BEND ?
$2\mathcal{J}/\hbar^2$ (MeV$^{-1}$)
$(h_{11/2})^2$ ALIGNED
0.08
0.16
0.24
0.32
0.40
0.48
0.56
0.64
(ROTATIONAL FREQUENCY)$^2$ $(\hbar\omega)^2$

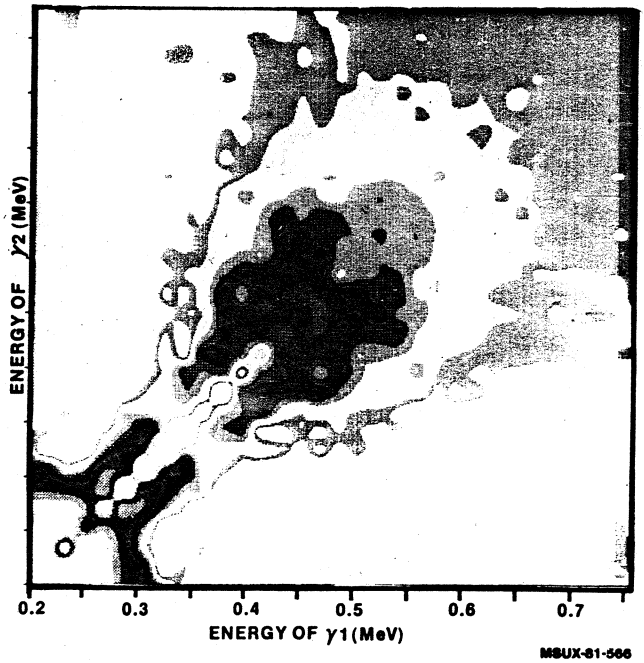
ENERGY OF γ2 (MeV)
0.2
0.3
0.4
0.5
0.6
0.7
ENERGY OF γ1 (MeV)
MSUX-81-566

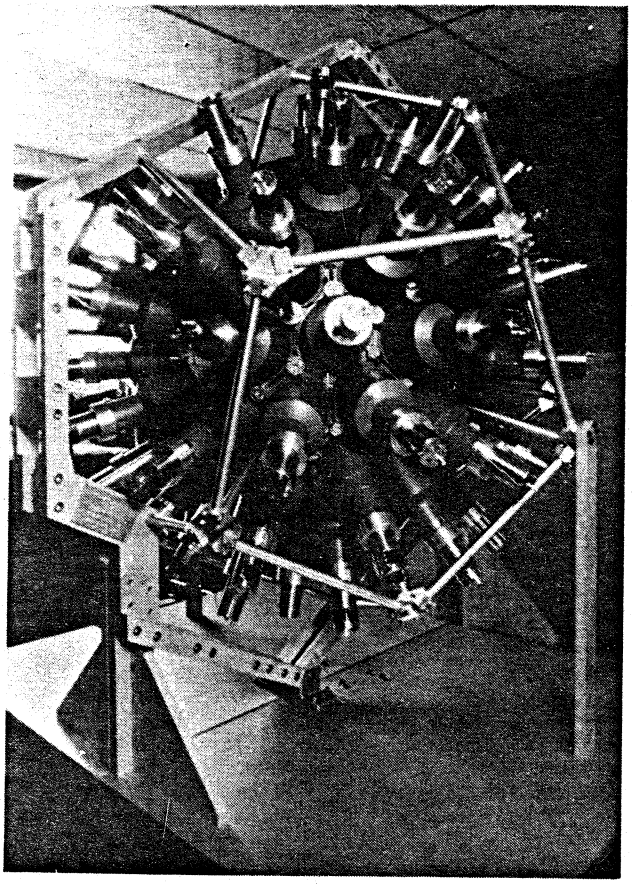

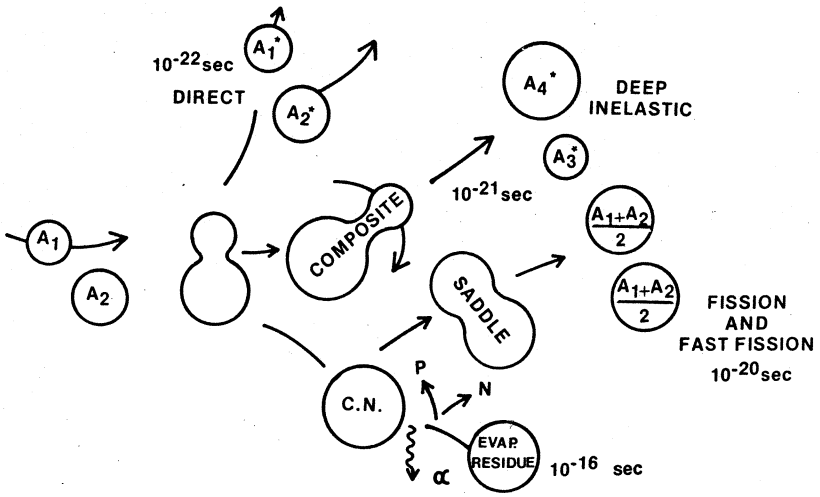
$10^{-22}$sec
DIRECT
$A_1^*$
$A_2^*$
$A_4^*$
DEEP INELASTIC
$A_3^*$
$10^{-21}$sec
$A_1$
$A_2$
COMPOSITE
$\frac{A_1+A_2}{2}$
SADDLE
$\frac{A_1+A_2}{2}$
FISSION AND FAST FISSION
$10^{-20}$sec
C.N.
P
N
EVAP. RESIDUE
α
$10^{-16}$ sec

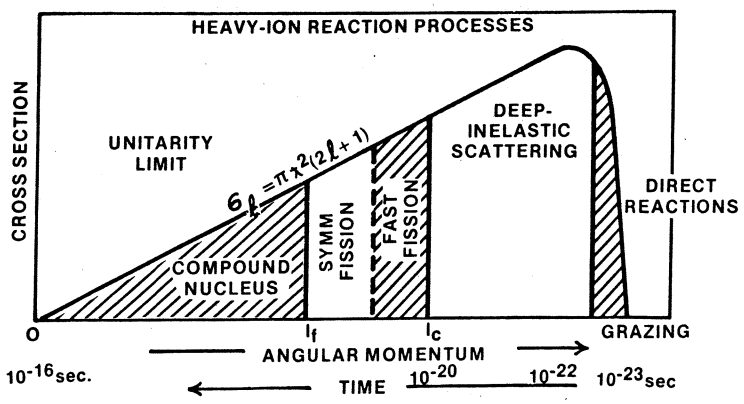
HEAVY-ION REACTION PROCESSES
CROSS SECTION
UNITARITY LIMIT
$\sigma_\ell = \pi\lambda^2(2\ell+1)$
DEEP-INELASTIC SCATTERING
DIRECT REACTIONS
COMPOUND NUCLEUS
SYMM FISSION
FAST FISSION
0
$\ell_f$
$\ell_c$
GRAZING
ANGULAR MOMENTUM
$10^{-16}$sec.
TIME
$10^{-20}$
$10^{-22}$
$10^{-23}$sec

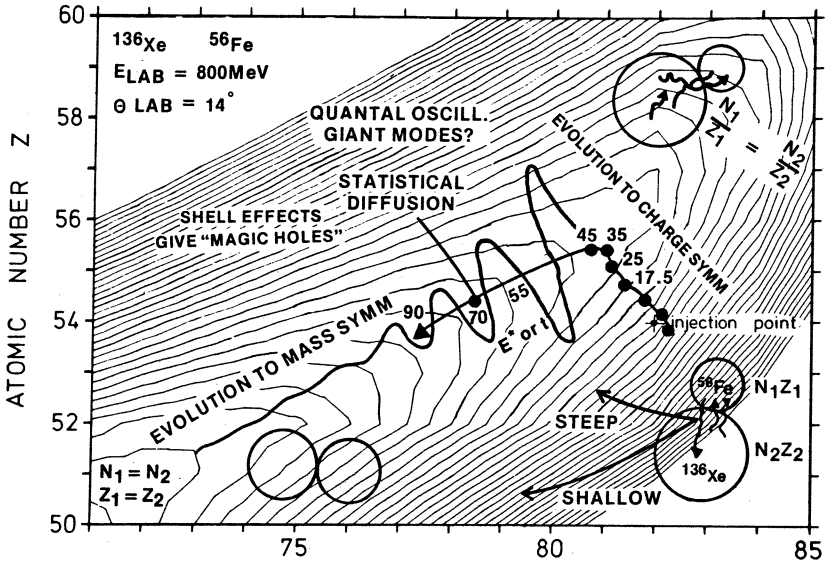


**POTENTIAL ENERGY SURFACE:**

$$\left[1-K\left(\frac{A-2Z}{A}\right)^2\right]\left(-a_vA+a_sA^{2/3}\right)+\frac{3}{5}\left[\frac{e^2z^2}{r_oA^{1/3}}\right]-\frac{\pi^2}{2}\left(\frac{e^2}{r_o}\right)\left(\frac{a}{r_o}\right)^2\frac{Z^2}{A}$$

**PROVIDES A DRIVING FORCE FOR EVOLUTION OF VARIOUS DEGREES OF FREEDOM AS A FUNCTION OF TIME.**

MSUX-81-447

MSUX-81-322

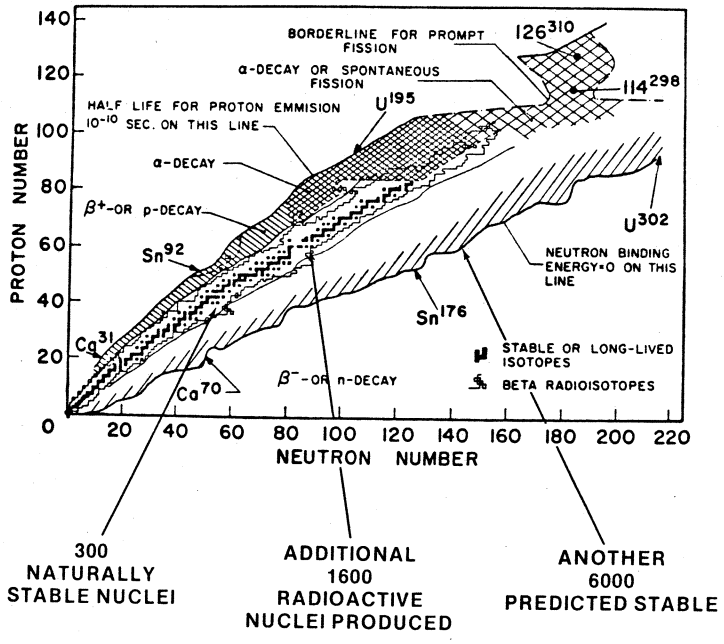


300 NATURALLY STABLE NUCLEI

ADDITIONAL 1600 RADIOACTIVE NUCLEI PRODUCED

ANOTHER 6000 PREDICTED STABLE

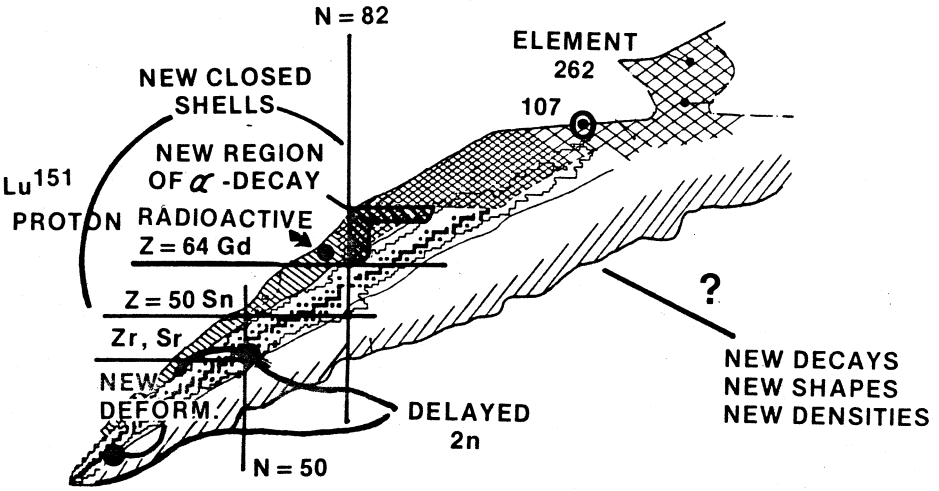


MSUX-81-557

MSUX-81-255

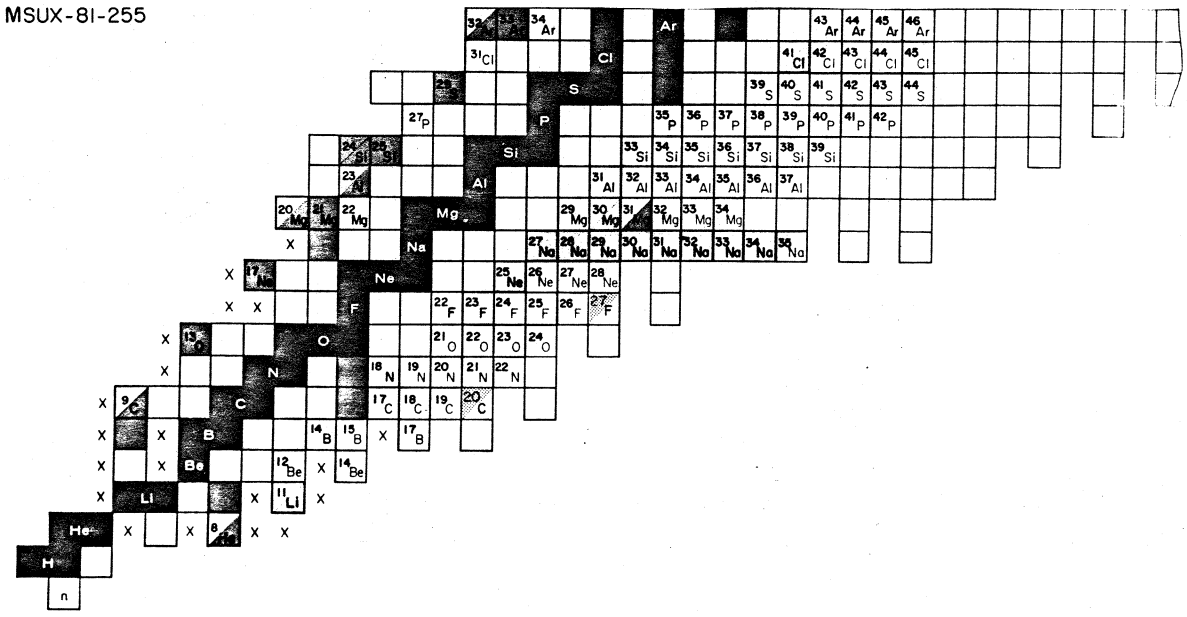

MSUX-81-328

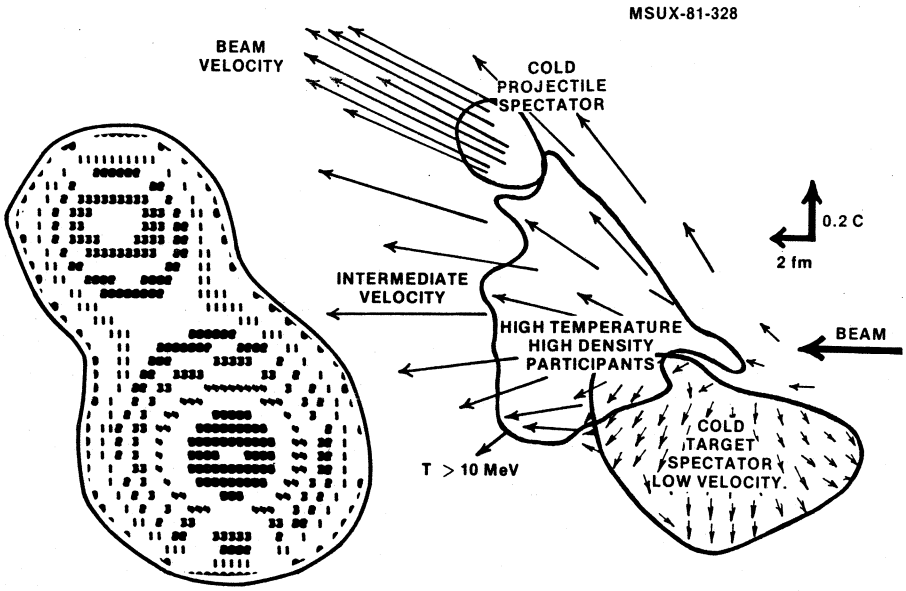


$^{16}O$ on Ca at 6 MeV/NUCLEON
DENISTY PROFILES IN
TIME DEPENDENT HARTREE FOCK
SLOW TIME EVOLUTION
MEAN FREE PATH ⟶ ∞

$^{20}Ne$ on U. at 400 MeV/NUCLEON
TEMPERATURE, DENSITY & VELOCITY PROFILES.
IN HYDRODYNAMICS
FAST TIME EVOLUTION
MEAN FREE PATH ⟶ 0

MSUX-81-320

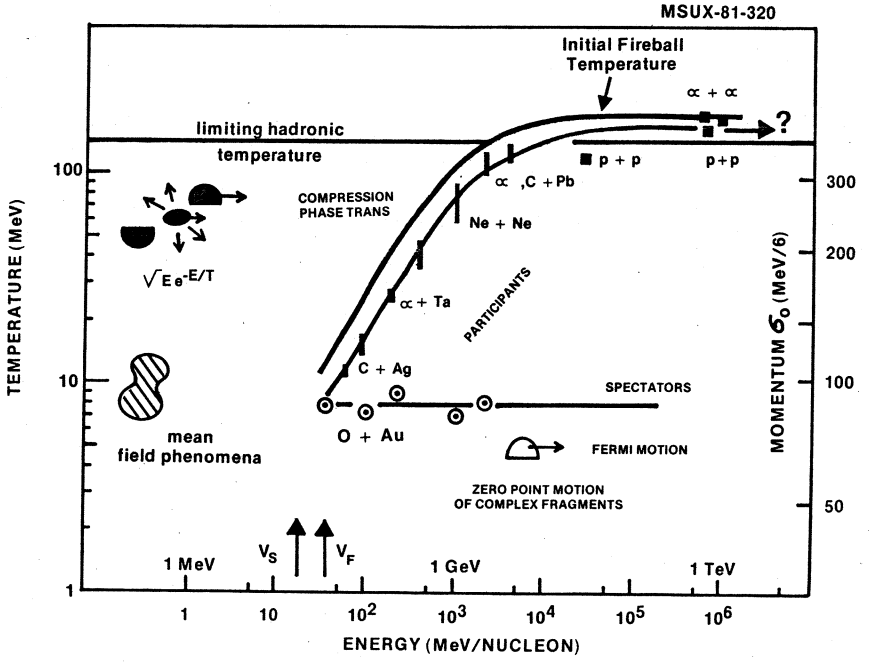

FIREBALL TEMPERATURE FOR SEVERAL
HADRONIC MASS SPECTRA

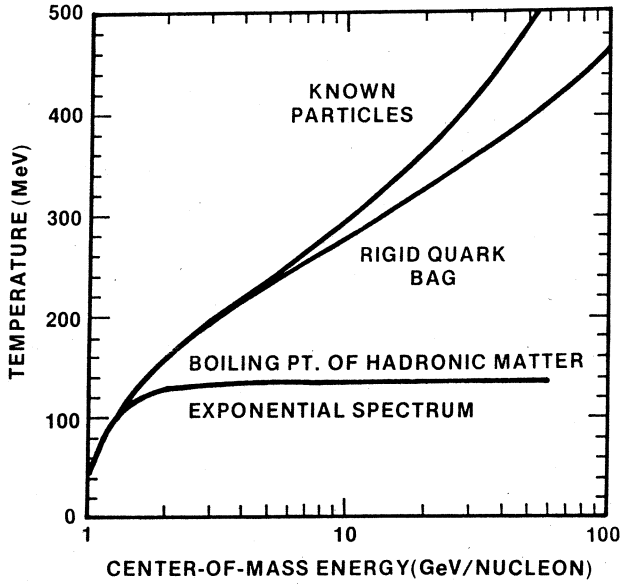


AN EXPONENTIAL HADRON SPECTRUM IS A FEATURE OF THE
OLD BOOTSTRAP MODEL IN WHICH

THE INTERATION
IS GENERATED BY REACTIONS BETWEEN BOUND STATES AND
RESONANCES, WHICH THEMSELVES ARE GENERATED BY THE INTER-
ACTION, WHICH

MSUX-81-450

MSUX-81-556

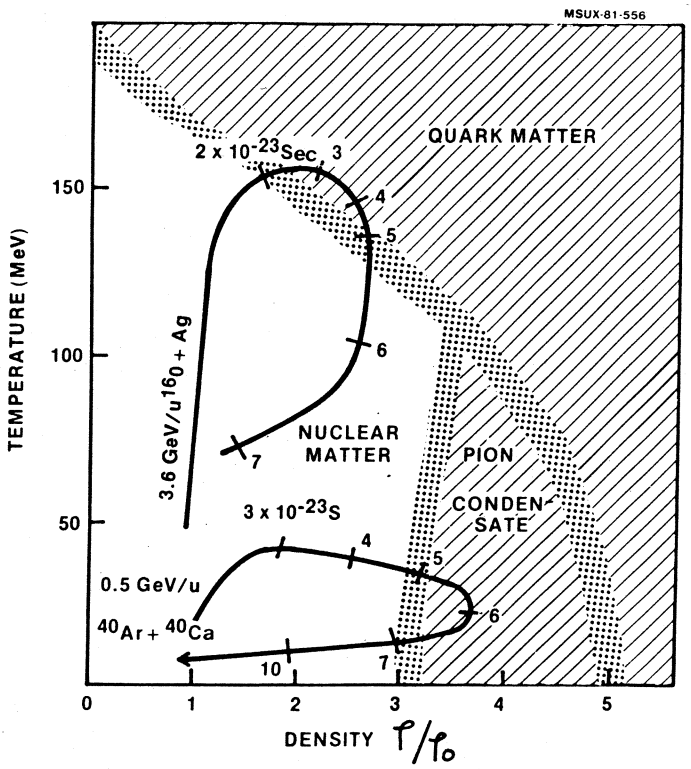

$^{20}$Ne + U ⟶ P 393 MeV/NUCLEON

HIGH MULTIPLICITY - CENTRAL COLLISION

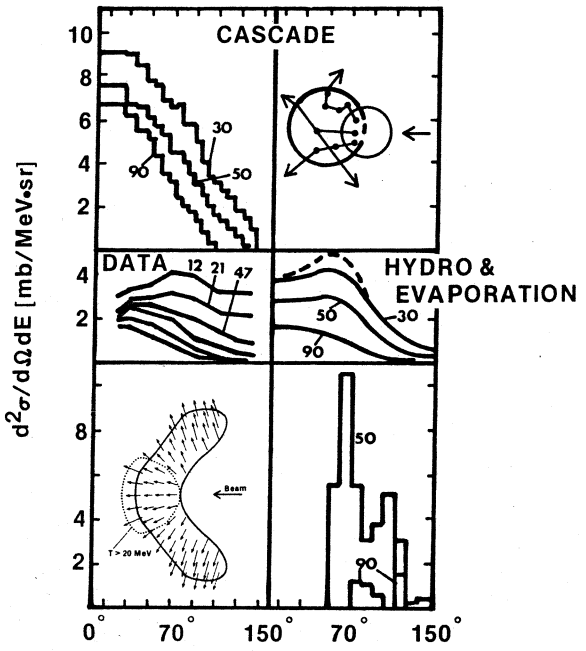


MSUX-81-451

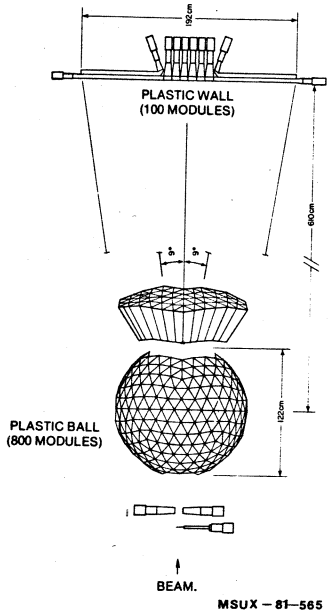


MSUX – 81–565

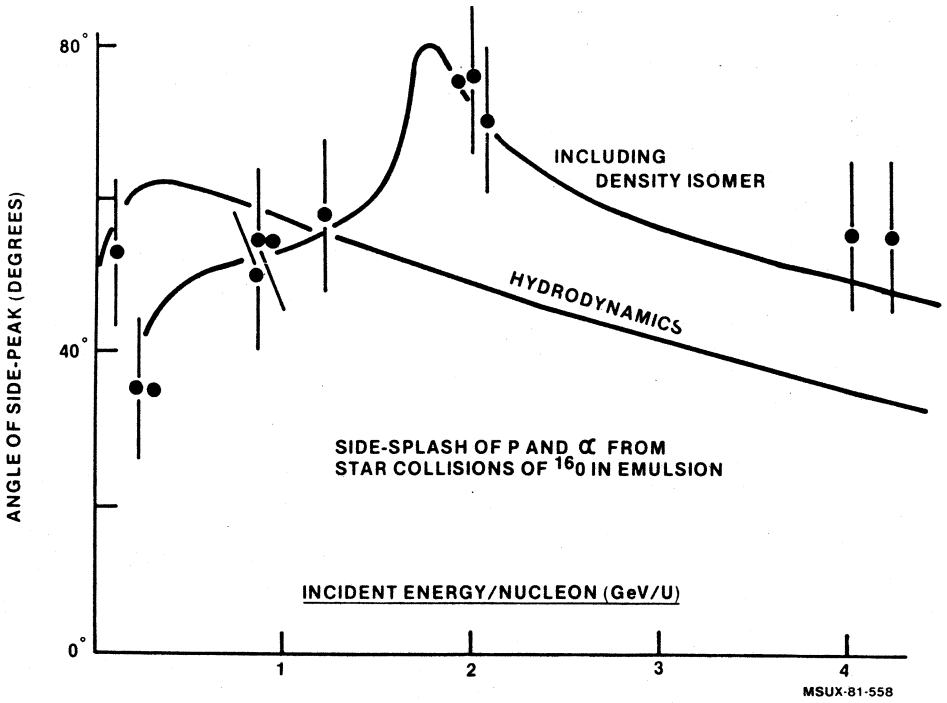


## ANOMALONS

INTERACTIONS OF Fe of 1.5 GeV/NUCLEON
IN AN EMULSION.

PRODUCES SERIES OF STARS.

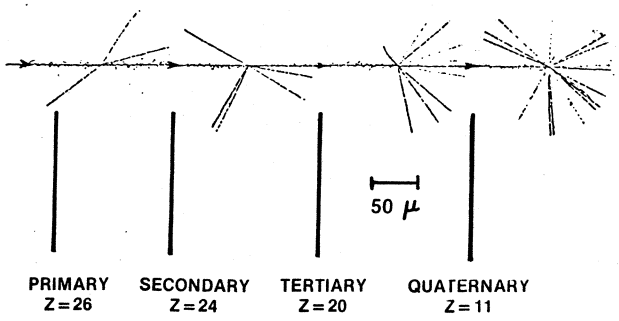


SOME SECONDARIES, TERTIARIES..... HAVE SHORTER INTERACTION LENGTHS THAN NORMAL PARTICLES OF SAME Z AND E.

RESULTS COMPATIBLE WITH 6% CONTRIBUTION OF ONE TENTH MEAN FREE PATH, OR 10 TIMES NORMAL CROSS SECTION: LIFETIME $> 10^{-10}$ sec

MSUX-81-449

MSUX-81-319

DEMON DEUTERONS

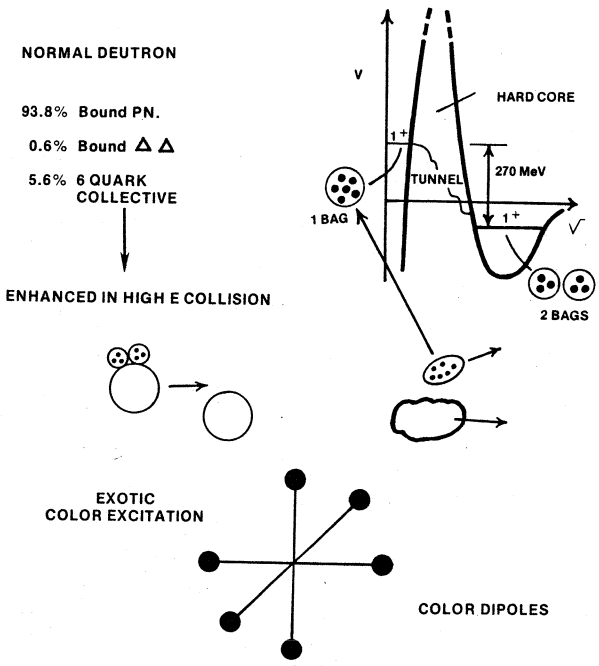


MSUX-81-327

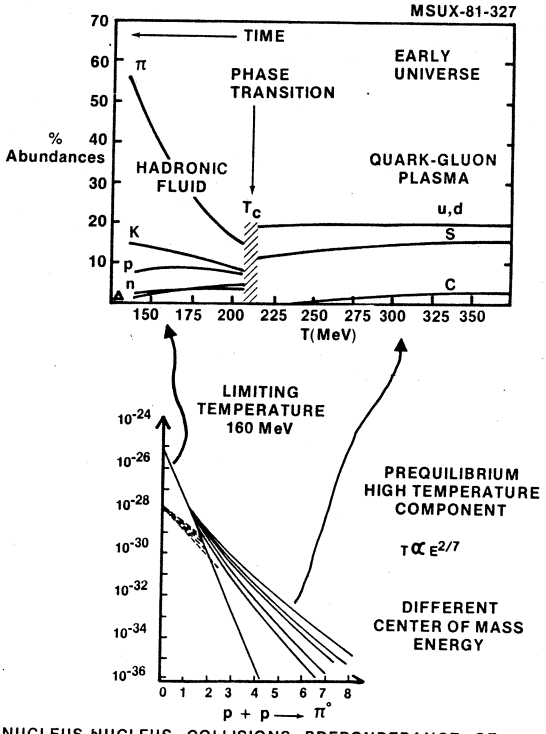


IN NUCLEUS-NUCLEUS COLLISIONS PREPONDERANCE OF $u + d$ QUARKS LEAD TO CHARACTERISTIC PRODUCTION RATIOS, e.g. $\bar{\Lambda} / \bar{p}$